Isotopic yields of neutron-rich nuclei from deep-inelastic reactions

S. J. Asztalos, I. Y. Lee, K. Vetter, B. Cederwall, R. M. Clark, M. A. Deleplanque, R. M. Diamond, P. Fallon, K. Jing, L. Phair, A. O. Macchiavelli, F. S. Stephens, and G. J. Wozniak
Nuclear Science Division, Lawrence Berkeley National Laboratory, Berkeley, California 94721

L. A Bernstein and D. P. McNabb
Physics Division, Lawrence Livermore National Laboratory, Livermore, California 94550

P. F. Hua and D. G. Sarantites
Washington University, St. Louis, Missouri 63130

J. X. Saladin
University of Pittsburgh, Pittsburgh, Pennsylvania 15260

C.-H. Yu
Physics Division, Oak Ridge National Laboratory, Oak Ridge, Tennessee 37830

J. A. Cizewski
Rutgers University, New Brunswick, New Jersey 08903
(Received 20 July 1999; published 1 December 1999)

We follow up on our earlier work involving a light projectile (^{48}Ca) to populate high spin states in neutron-rich nuclei with results from experiments involving a heavier projectile (^{154}Sm) for the purposes of studying isotopic yields. These yields, which in some cases were measurable down to a level of 0.1% of the total reaction cross section, are presented from three separate reactions. A trend in the isotopic yields towards N/Z equilibration is observed in one experiment having a large disparity in N/Z ratios between the projectile and target. In the two other reactions, where the N/Z driving force is less pronounced, the yields are instead clustered around the projectile and target nuclei. We present correlated projectilelike and targetlike fragment isotopic yields derived from γ-γ coincidences, a technique that enables one to partition the yield of an isotope according to the amount of neutron evaporation. Using this method we find that for the zero-neutron evaporation channel transfer occurs predominantly into the light fragment, consistent with the nature of the deep-inelastic mechanism. We further find that multiple-neutron evaporation contributes substantially to the yields of the isotopes.

PACS number(s): 21.10.Gv, 25.70.Hi, 27.40.+z, 27.70.+q

I. INTRODUCTION

Neutron-rich nuclei may possess novel features such as modified residual interactions, a neutron skin, or exotic modes of excitation. A challenge lies, however, in their production, since the majority of reaction mechanisms do not produce neutron-rich isotopes. By contrast, deep-inelastic reactions can access nuclei with appreciably higher N/Z ratios [1], thus permitting the study of otherwise inaccessible nuclei. Furthermore, due to its potential for substantial energy dissipation and angular momentum generation, the deep-inelastic reaction mechanism has begun to play a more prominent role in high-spin nuclear structure studies [2–5]. A typical approach, exemplified by the recent experiment ^{64}Ni+^{130}Te at 350 MeV [3], involves a target sufficiently thick to stop all recoiling reaction fragments. In that experiment new transitions were found in the four-neutron transfer product ^{68}Ni whose half-life of 19 s precludes study by Coulomb excitation in a conventional accelerator facility.

Our use of a thin target distinguishes the experiments described in this paper from thick-target experiments in that we rely on kinematic reconstruction of the event and Doppler-correction of the γ rays to identify the reaction products. With this technique the cross sections for producing an isotope are known at a particular energy. Additionally, the thin-target technique is impervious to Doppler broadening of the fastest (highest spin) transitions caused by rapid slowing in a thick target. In an experiment designed to exploit the potential of this reaction mechanism for producing high-spin states in neutron-rich nuclei we discovered 39 new γ ray transitions in eight neutron-rich ytterbiumlike nuclei using ^{48}Ca +^{176}Yb at 250 MeV [6]. In that experiment we were able to measure rotational states as high as $12\hbar$ in ^{178}Yb. By comparison, compound nucleus reactions cannot access Yb isotopes heavier than ^{168}Yb. In this paper we extend our earlier work by exploring the impact of changes in the makeup of the projectile and target on the isotopic yields. Accordingly, we chose the reaction ^{154}Sm+^{176}Yb at 949 MeV, followed by the reaction ^{154}Sm+^{208}Pb at 1 GeV. (These experiments are referred to as ^{154}Sm+^{176}Yb and ^{154}Sm+^{208}Pb, respectively, throughout the remainder of this paper, whereas our previous experiment is referred to as ^{48}Ca+^{176}Yb.) The reaction ^{154}Sm+^{176}Yb was designed to explore the implications of going from a light beam (^{48}Ca) to the heaviest beam that the 88-in. cyclotron at the Lawrence Berkeley National Laboratory was capable of producing at an energy of 6 MeV/

 ©1999 The American Physical Society

TABLE I. Experimental parameters relevant for determining the isotopic yields.

	Target thickness [mg/cm^2]	I [p-pA]	Δt [hrs]	$\Delta\Omega$ [mb/sr]
^{48}Ca+^{176}Yb	1.0	3.25	82	1048
^{154}Sm+^{176}Yb	1.0	0.8	47	1590
^{154}Sm+^{208}Pb	1.0	0.34	50	1454

nucleon, while using the same target (^{176}Yb) as in our earlier work. The experiment ^{154}Sm+^{208}Pb was intended to study the consequences of using a target with the highest N/Z ratio of any stable, commercially available target, while keeping the same projectile (^{154}Sm) as in the preceding experiment. To minimize the influence of beam energy on the isotopic yields all three experiments were run at an energy of roughly 6 MeV/nucleon.

The results of these experiments fall into two general categories: the isotopic yields of the various reaction products and the spin yields, i.e., how the isotopic yields vary as a function of spin. In this paper we address the isotopic yields. In Sec. II we describe the technique used to convert γ-ray energies into isotopic yields. In Sec. III A we present the yields from the experiments and discuss the results in terms of N/Z and Q-value considerations. Finally, in Sec. III B we compare these results with the results obtained via cross-gating.

In a previous paper we presented spin yields from these reactions [7]. We refer the interested reader to that paper and Ref. [6] for a complete description of the experimental setup.

II. YIELD DETERMINATION

In each experiment a silicon strip detector was placed downstream from the target and centered around the grazing angle to enhance the yield coming from large energy loss events. For the reactions ^{48}Ca+^{176}Yb and ^{154}Sm+^{208}Pb it was further possible to kinematically select events off-line in which the projectilelike fragment hit the silicon strip detector, again for the same purpose. An event was defined by the coincident measurement of a fragment at the silicon strip detector and two γ rays detected by GAMMASPHERE.

Isotopic yields were determined from the area of the lowest spin peak of a nucleus in the γ-ray energy spectrum. In the case of weakly populated isotopes it was necessary to gate on the lowest lying transition and use the second lowest transition in order to determine the yield. The peak area A obtained in this way is dependent upon the target thickness μg/cm^2, beam current I and duration of the experiment Δt. Representative values for these experimental parameters for each of the three experiments can be found in Table I. The solid angles $\Delta\Omega$ subtended by the silicon strip detector (as seen from the target) can be derived analytically due to the cylindrical geometry of the experimental setup. These values are also included in Table I. The differential cross section obtained in this way must still be corrected for the absolute efficiency of GAMMASPHERE at the energy of the fitted

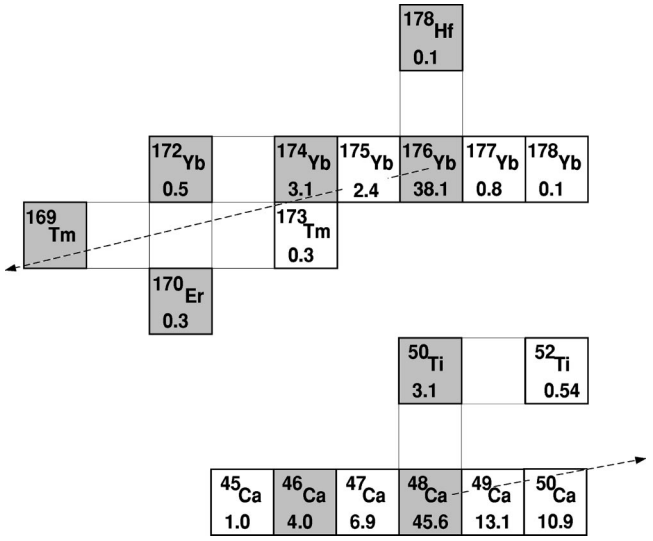

FIG. 1. Production cross sections (mb/sr) from ^{48}Ca+^{176}Yb corresponding to Ca-like nuclei striking the silicon strip detector ($55° \leqslant \theta_{Ca} \leqslant 67°$) from single gates in a matrix. The shaded boxes identify stable nuclei, while the dashed lines reflect an N/Z ratio of approximately 1.49 corresponding to the compound system.

peak (and the energy of the gate used to derive the spectrum from which the peak fit is made, if necessary). This method produced the isotopic yields in Figs. 1 through 3. Due to the difficulty in resolving peaks in the spectrum, the yields for ^{154}Sm+^{176}Yb were obtained by double-gating three-fold data.

By studying the γ rays of the projectilelike (targetlike) fragment coincident with the targetlike (projectilelike) γ rays, one explores correlations between the nuclei populated in the reaction (cross-gating). Matrices containing cross-gated yields were produced for ^{48}Ca+^{176}Yb and ^{154}Sm +^{208}Pb data with one of the axes corresponding to γ-ray energies corrected for the projectilelike fragments, and the other axis corrected for the targetlike fragments. The technique of cross-gating is especially useful for identifying a nucleus when no levels are known in its level scheme, or if the levels in one nucleus lie too close in energy with another to permit unambiguous identification by normal coincidence techniques. An example of the latter was the identification of ^{170}Er via cross-gating on ^{54}Ti transitions from ^{48}Ca+^{176}Yb

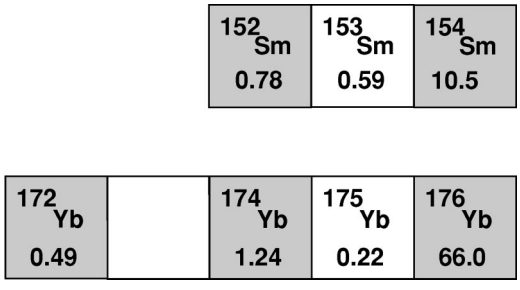

FIG. 2. Production cross sections (mb/sr) from ^{154}Sm+^{176}Yb corresponding to either Sm-like nuclei or Yb-like nuclei hitting the silicon strip detector and emitting the γ rays. Due to the similarity in masses, both situations approximately correspond to $45° \leqslant \theta_{recoil} \leqslant 63°$.

^{152}Sm	^{153}Sm	^{154}Sm	^{155}Sm	^{156}Sm
1.0	1.0	16.2	0.2	0.15

^{206}Pb	^{207}Pb	^{208}Pb	^{209}Pb
2.1	3.8	6.1	0.2

FIG. 3. Production cross sections (mb/sr) from ^{154}Sm+^{208}Pb corresponding to Sm-like nuclei hitting the silicon strip detector ($45° \leqslant \theta_{Sm} \leqslant 65°$) from single gates in a matrix.

data. ^{170}Er has rotational transitions (from the 2^+ to the 8^+ states) that are virtually identical in energy to the much stronger transitions in ^{172}Yb.

Figure 4 illustrates a typical cross-gated spectrum from ^{154}Sm+^{208}Pb for Sm-like nuclei, in this case obtained by gating on the $3^- \rightarrow 0^+$ transition in ^{208}Pb at 2614 keV. This cross-gated spectrum brings back much of the known rotational band in ^{154}Sm plus two low-lying transitions in ^{153}Sm. As one example of measuring cross-gated yields,

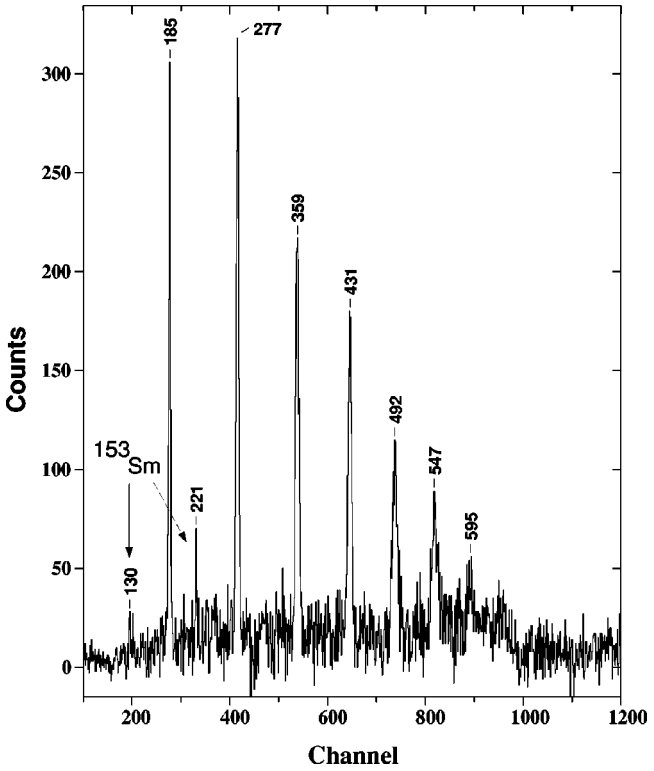

FIG. 4. A cross-gated spectrum of Sm-like nuclei from a gate on a Doppler-corrected ^{208}Pb transition at 2614 keV. Prominent in this spectrum are the ground state rotational band in ^{154}Sm (up to a spin of 16^+) and two low-lying transitions in ^{153}Sm. The cross-gated yields for ^{153}Sm and ^{154}Sm in coincidence with ^{208}Pb are derived from the peaks 130 and 185 keV, respectively. Transition energies shown above the peaks are derived from a calibration of 0.667 keV/channel.

	^{153}Sm	^{154}Sm	^{155}Sm	^{156}Sm
^{206}Pb		0.15		0.19
^{207}Pb	0.04	0.25	0.28	
^{208}Pb	0.06	1.0		
^{209}Pb	0.03			
Q (MeV)	-4.03	0.0	-1.56	-1.05

FIG. 5. Cross-gated yields for ^{154}Sm+^{208}Pb for Sm nuclei hitting the silicon strip detector. All values are normalized to the cross-gated yield of the $2^+ \rightarrow 0^+$ transition in ^{154}Sm. The diagonal contains yields for reaction partners experiencing no neutron evaporation, while entries off the diagonal reflect varying degrees of neutron evaporation. Missing entries below the diagonal are inaccessible via this reaction, while those above the diagonal imply intensities too low to measure. The ground state Q values for the diagonal entries are listed at the bottom of the figure.

peaks at 130 keV and 185 keV (corresponding to ^{153}Sm and ^{154}Sm, respectively) are fitted. This measurement resulted in the entries in the third row of the cross-gated yield matrix for ^{154}Sm+^{208}Pb in Fig. 5, along with the yields from other channels for this reaction. Most of the yields in this figure come from gates placed on γ rays from Pb-like fragments as these (single-particle) transitions are generally better isolated than the (rotational) Sm transitions. All values in this matrix have been normalized to the yield of the $2^+ \rightarrow 0^+$ in ^{154}Sm resulting from a gate on the $3^- \rightarrow 0^+$ in ^{208}Pb. A similar methodology was applied to the ^{48}Ca+^{176}Yb data to produce Fig. 6. In these figures, the Q values for the diagonal reaction partners are shown beneath the correlated yield data. Empty entries in the lower right triangle of these matrices reflect

	^{174}Yb	^{175}Yb	^{176}Yb	^{177}Yb	^{178}Yb
^{46}Ca	0.011	0.024	0.034	0.019	0.031
^{47}Ca	0.013	0.083	0.067	0.041	
^{48}Ca	0.056	0.081	1.0		
^{49}Ca	0.074	0.090			
^{50}Ca	0.119				
Q (MeV)	-1.19	-1.17	0.0	-4.37	-4.21

FIG. 6. Cross-gated yields for ^{48}Ca+^{176}Yb for Ca nuclei hitting the silicon strip detector. See the caption to Fig. 5 for a discussion.

TABLE II. The first, second, and third columns identify the relevant experiment and the atomic masses of the projectile and target nuclei, respectively. The fourth column gives the N/Z ratio of the (hypothetical) compound nucleus. The fifth and sixth columns specify the N/Z ratios of the projectilelike and targetlike nuclei, respectively. Of these nuclei, only ^{210}Pb escaped detection. The last column gives the Q value for the corresponding set of transfer products.

Expt.	A_{pl}	A_{tl}	$(N/Z)_{cn}$	$(N/Z)_{pl}$	$(N/Z)_{tl}$	Q
	^{46}Ca	^{178}Yb	-	1.30	1.54	−4.9
	^{47}Ca	^{177}Yb	-	1.35	1.53	−4.4
	^{49}Ca	^{175}Yb	-	1.45	1.50	−1.7
^{48}Ca+^{176}Yb	^{48}Ca	^{176}Yb	1.49	1.40	1.51	0
	^{50}Ca	^{174}Yb	-	1.50	1.48	−1.2
	^{50}Ti	^{174}Er	-	1.27	1.55	5.8
	^{52}Ti	^{172}Er	-	1.36	1.53	8.2
	^{153}Sm	^{177}Yb	-	1.46	1.53	−2.4
	^{152}Sm	^{178}Yb	-	1.45	1.54	−1.5
^{154}Sm+^{176}Yb	^{154}Sm	^{176}Yb	1.50	1.48	1.51	0
	^{155}Sm	^{175}Yb	-	1.50	1.50	−1.1
	^{156}Sm	^{174}Yb	-	1.52	1.48	0.4
	^{152}Sm	^{210}Pb	-	1.45	1.56	−4.7
	^{153}Sm	^{209}Pb	-	1.46	1.55	−4.0
^{154}Sm+^{208}Pb	^{154}Sm	^{208}Pb	1.51	1.48	1.53	0
	^{155}Sm	^{207}Pb	-	1.50	1.52	−1.6
	^{156}Sm	^{206}Pb	-	1.52	1.51	−1.1

products that cannot be produced in these reactions, whereas gaps elsewhere imply intensities too weak to measure.

III. RESULTS AND DISCUSSION

Previous work has demonstrated that one experimental signature of the deep-inelastic process is the tendency for the reaction products to be enhanced in the vicinity of the N/Z ratio of the composite system [8]. Consequently, if both projectile and target are neutron-rich, the same will tend to hold for the resultant products. Beyond these generalities, little is known about how the product distribution is influenced by the masses of the projectile and target pair or on the difference in the N/Z ratios between them. Another uncertainty is the degree to which neutron evaporation will conspire to lower the N/Z ratios of the final products. To systematically study nuclear structure in the most neutron-rich nuclei we sought to address these questions using both light and heavy projectiles on heavy rare-earth by nuclei.

A. Isotopic yields

To aid in the interpretation of the yield patterns, the N/Z and Q values for representative reaction product pairs are given in Table II. The fourth column of this table gives the N/Z ratio of the composite system formed from the projectile and target nuclei, while the fifth and sixth columns give the N/Z ratios of the projectilelike and targetlike fragments for each reaction, respectively.

The isotopic yields from the reaction ^{48}Ca+^{176}Yb are shown in Fig. 1. The trends in the isotopic yields for this reaction can be understood in terms of the basic characteristics of deep-inelastic reactions outlined above. In this reaction the driving force for producing neutron-rich Ca nuclei is very favorable as is reflected by the large yields of $^{48-50}$Ca. By contrast, $^{45-47}$Ca, which have N/Z ratios in a direction opposite from the composite system, all have yields that are lower than those for the neutron-rich isotopes. For the Yb isotopes, the N/Z driving force is less pronounced but favors neutron-deficient nuclei. The production of $^{177-178}$Yb reflects the stochastic nature of the deep-inelastic mechanism, where variances give rise to products opposed by both the N/Z driving force and negative Q values [9]. By contrast, a multiple-nucleon transfer product, such as ^{169}Tm, which has a large negative Q value, is an unambiguous example of the deep-inelastic process since it clearly cannot be produced by quasielastic transfer. The dashed lines in Fig. 1 approximate $N/Z=1.49$ (the approximate N/Z ratio that would result from the fusion of ^{48}Ca and ^{176}Yb). For Yb-like nuclei this line lies along the line of β stability, and the observed yields follow this line. For Ca-like nuclei this same line points away from the line of β stability towards the neutron-rich line, again in agreement with the observed yields.

Figures 2 and 3 show the isotopic yields for the reactions ^{154}Sm+^{176}Yb and ^{154}Sm+^{208}Pb reactions, respectively. For these two reactions the N/Z ratios are similar between the projectilelike and targetlike products, hence N/Z equilibration is less important. As with the reaction ^{48}Ca+^{176}Yb, most of the cross section resides in the inelastic excitation of the projectile and target, as is to be expected with particle detection at the grazing angle. For the reaction ^{154}Sm+^{208}Pb nucleon transfer into the projectile (out of the target) is again favored, which accounts for the yields of the heavy Sm and light Pb nuclei populated in the reaction. Several factors likely contributed to the absence of heavy Sm products from the reaction ^{154}Sm+^{176}Yb, the most important being the inability to measure intensities on the order of 1% of the total reaction cross section due to the significant Doppler-broadening of the peaks. The inability to distinguish between the various kinematic solutions also contributed to this problem.

B. Correlated yields

Since the deep-inelastic mechanism involves large amounts of energy damping, neutron (and to a lesser extent proton) evaporation is expected. Therefore, the primary isotopic yields are distorted by neutron evaporation towards neutron-deficient nuclei. Correlated yields, by contrast, contain information about the amount of neutron evaporation that has occurred in populating a particular reaction pair. For example, the diagonal elements of the cross-gated yield matrices in Figs. 5 and 6 reflect the zero-neutron evaporation channels for the various reaction products. For these channels there is no ambiguity due to neutron evaporation and we confirm the results obtained from the raw yields, e.g., that transfer into the lighter projectile is strongly favored. From these figures it is also seen that one- and multiple-neutron

evaporation channels contribute substantially to the yields of the isotopes. This is seen most clearly in the relative correlated isotopic yield of ^{174}Yb, which is obtained by summing along the first column of Fig. 6. The yield of ^{174}Yb is dominated by direct population in coincidence with ^{50}Ca, but also has increasing contributions from $^{46-49}$Ca, corresponding to the loss of one to four neutrons. On average, about one neutron is emitted when ^{174}Yb is produced. A similar breakdown can be made concerning the yield of ^{46}Ca, which is comprised of contributions from $^{174-178}$Yb. Here the zero-neutron evaporation contribution to the yield of ^{46}Ca is exceeded by the contribution from the two-neutron evaporation channel. Unfortunately, the total yield of any of the final reaction products comes from both direct and indirect (neutron evaporation) processes, hence ambiguity arises about the actual path that the reaction products took in making products off the diagonal. This observation precludes extracting the direct component of the yield other than for the zero-neutron evaporation channel from the correlated yields.

The sum of the diagonal elements gives the total yield for the zero-neutron evaporation channels. The next off-diagonal elements represent one-neutron evaporation channels, and so on. The cross-gated yields for ^{48}Ca+^{176}Yb and ^{154}Sm+^{208}Pb were summed along these respective diagonals and plotted in Fig. 7. These data have been normalized to the zero-neutron emission yields from ^{48}Ca+^{176}Yb. The close agreement for one- and two-neutron emission is likely a reflection of the similar one- and two-neutron binding energies of ^{48}Ca and ^{208}Pb. The comparative flatness of the curve for ^{48}Ca+^{176}Yb for one and more neutron transfer is another indication of the deep-inelastic process since multiple neutron evaporation is additional evidence of the substantial energy dissipation expected from deep-inelastic processes.

Few cross-gated coincidences were seen in the reaction ^{154}Sm+^{176}Yb. This may be attributed to the Doppler-broadening already mentioned, or may have a more fundamental explanation, such as the large intrinsic deformations of both the projectilelike and targetlike nuclei in this reaction.

IV. CONCLUSIONS

Thin-target deep-inelastic experiments provide a selective approach for studying neutron-rich nuclei by means of γ-ray spectroscopy. In three separate experiments isotopic yields were obtained and yields as low as 0.1 mb/sr were measured in the case of ^{178}Yb. In instances where the difference between the N/Z ratios of the projectile and target is large the yield patterns tend to fall along the line dictated by the N/Z ratio of the composite system. When the N/Z ratio favors neutron transfer—as is the case with the reaction ^{48}Ca + ^{176}Yb—the yields can be appreciable. This is best seen by the two-neutron transfer yields into ^{48}Ca. This result should open the door to the study of a wide variety of light, very neutron-rich isotopes. For the heavy reaction partner the driving force is away from neutron richness. Still, since nucleon transfer in the deep-inelastic process is a stochastic process, yields in nuclei that defy these driving forces can be appreciable, as was seen by the production of $^{177-178}$Yb.

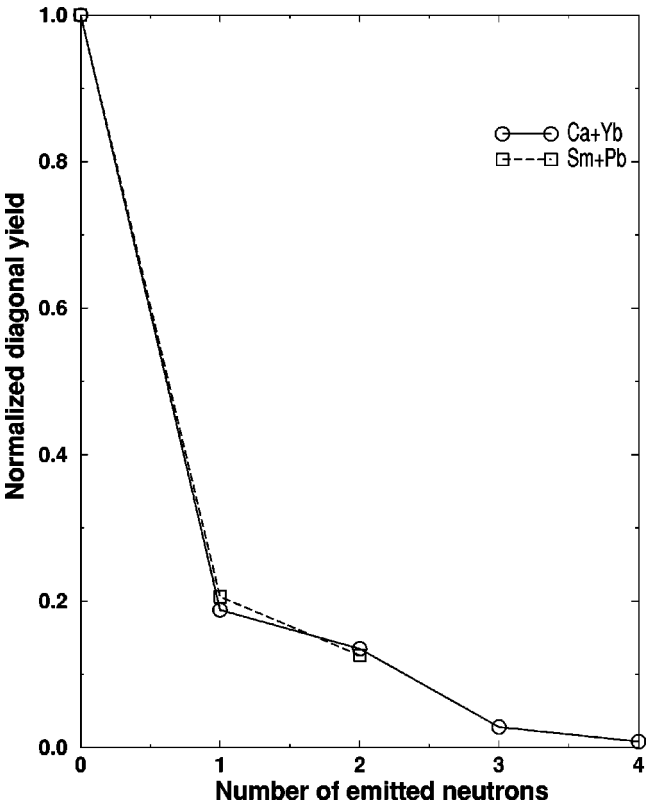

FIG. 7. Cross-gated sums along the diagonals of Figs. 5 and 6 from the reactions ^{154}Sm+^{208}Pb and ^{48}Ca+^{176}Yb, respectively. The data are normalized to the zero-neutron transfer emission yields from ^{48}Ca+^{176}Yb.

On the other hand, if the N/Z ratios of the projectile and target are similar, as they were in the reactions ^{154}Sm+^{176}Yb and ^{154}Sm+^{208}Pb, nuclei in the vicinity of the projectile and target nucleus are predominantly populated. Nonetheless, the yields are sufficient to permit study of neutron-rich projectilelike nuclei by this method.

In these experiments the technique of cross-gating provides for a precise measurement of the zero-neutron evaporation yields. We find that the yields for product pairs that are favored on the basis of N/Z and Q value considerations are considerably enhanced. Furthermore, multiple neutron evaporation is shown to substantially contribute to the isotopic yields.

The lack of neutron transfer into the projectile or target in ^{154}Sm+^{176}Yb serves as a reminder that in reactions where the recoiling velocities approach 10% of the speed of light Doppler broadening is significant, thus making weak channels hard to find. This problem can be solved by using more highly segmented particle and γ-ray detectors.

ACKNOWLEDGMENTS

We would like to express our gratitude to the staff of the 88-inch cyclotron for the development of the ^{154}Sm beam used in both the ^{154}Sm+^{176}Yb and ^{154}Sm+^{208}Pb experiments. This work was supported by the U.S. Department of Energy, Nuclear Science Division, under Contract No. DE-AC03-76SF00098.

[1] V. V. Volkov, Phys. Rep., Phys. Lett. **C2**, 93 (1978).
[2] H. Takai *et al.*, Phys. Rev. C **38**, 1247 (1988).
[3] R. Broda *et al.*, Phys. Rev. Lett. **74**, 868 (1995).
[4] P. H. Regan *et al.*, Phys. Rev. C **55**, 2305 (1997).
[5] K. Vetter *et al.*, Phys. Rev. C **56**, 2316 (1997).
[6] I. Y. Lee *et al.*, Phys. Rev. C **56**, 753 (1997).
[7] S. J. Asztalos *et al.*, Phys. Rev. C **60**, 044307 (1999).
[8] W. Krolas *et al.*, Acta Phys. Pol. B **27**, 493 (1996).
[9] R. Planeta *et al.*, Phys. Rev. C **38**, 195 (1988).